Cancer Cell
Article

TEM8/ANTXR1 Blockade Inhibits Pathological Angiogenesis and Potentiates Tumoricidal Responses against Multiple Cancer Types

Amit Chaudhary,[1] Mary Beth Hilton,[1,2] Steven Seaman,[1] Diana C. Haines,[3] Susan Stevenson,[4] Peter K. Lemotte,[4] William R. Tschantz,[4] Xiaoyan M. Zhang,[4,5] Saurabh Saha,[4,5] Tony Fleming,[4] and Brad St. Croix[1,*]
[1]Tumor Angiogenesis Section, Mouse Cancer Genetics Program, National Cancer Institute (NCI), National Institutes of Health (NIH), Frederick, MD 21702, USA
[2]Basic Research Program
[3]Veterinary Pathology Section, Pathology/Histotechnology Laboratory
Science Applications International Corporation (SAIC), NCI, NIH, Frederick, MD 21702, USA
[4]Novartis Institutes for BioMedical Research, Cambridge, MA 02139, USA
[5]Present address: BioMed Valley Discoveries, Kansas City, MO 64111, USA
*Correspondence: stcroix@ncifcrf.gov
DOI 10.1016/j.ccr.2012.01.004

SUMMARY

Current antiangiogenic agents used to treat cancer only partially inhibit neovascularization and cause normal tissue toxicities, fueling the need to identify therapeutic agents that are more selective for pathological angiogenesis. Tumor endothelial marker 8 (TEM8), also known as anthrax toxin receptor 1 (ANTXR1), is a highly conserved cell-surface protein overexpressed on tumor-infiltrating vasculature. Here we show that genetic disruption of *Tem8* results in impaired growth of human tumor xenografts of diverse origin including melanoma, breast, colon, and lung cancer. Furthermore, antibodies developed against the TEM8 extracellular domain blocked anthrax intoxication, inhibited tumor-induced angiogenesis, displayed broad antitumor activity, and augmented the activity of clinically approved anticancer agents without added toxicity. Thus, TEM8 targeting may allow selective inhibition of pathological angiogenesis.

INTRODUCTION

Solid tumors have an insidious ability to nourish their own expansive growth by evoking the sprouting of new blood vessels, or angiogenesis, from nearby vessels of neighboring nonmalignant tissues. Upon vascularization, tumor blood vessels supply tumor cells with vital oxygen and nutrients needed to support their continued growth, and provide a key escape route for metastasis. Due to their critical role in promoting tumor growth and metastasis, tumor blood vessels have become a major target of current anticancer therapy (Kerbel, 2008). Vascular endothelial growth factor (VEGF) and its receptor, VEGFR2, represent the most advanced targets of current antiangiogenic therapy, and agents that target the VEGF/VEGFR2 axis have been clinically approved to treat patients with colon, lung, brain, and kidney cancer (Brastianos and Batchelor, 2010; Kerbel, 2008). Although therapies targeting VEGF/VEGFR2 have improved the efficacy of current anticancer treatment strategies, angiogenesis is seldom completely halted, and both angiogenesis and tumor growth inevitably progress in the face of continued therapy. Furthermore, in addition to its well-known role in physiological angiogenesis of the adult, for example, during menstruation, ovulation, and wound healing, VEGF is also widely expressed in nonangiogenic normal adult tissues, where it plays critical roles in normal adult physiology (Maharaj and D'Amore, 2007). For example, it is required for normal kidney filtration (Eremina

Significance

Inhibiting angiogenesis has become an important adjunct to traditional anticancer therapy, but current antiangiogenic agents, including VEGF/VEGFR2 pathway inhibitors, disrupt normal physiological processes and are associated with an increasing number of adverse side effects. TEM8 is an appealing target for selective inhibition of tumor angiogenesis because it is functionally required for optimal tumor angiogenesis and growth but dispensable for normal development and physiological angiogenesis. Function-blocking antibodies specific to the extracellular domain of TEM8 blocked pathological angiogenesis and tumor growth and augmented the activity of various classes of anticancer agents, including VEGFR inhibitors. Thus, targeting TEM8 on tumor vasculature may provide opportunities for the selective blockade of cancer and other diseases dependent on pathological angiogenesis.

et al., 2006), preventing neural degeneration (Oosthuyse et al., 2001), and maintaining functional hematopoietic, endocrine, and skeletal systems (Sung et al., 2010). Given the pleiotropic activities of the VEGF pathway, it is not surprising that anti-VEGF/VEGFR2 therapies are associated with a number of toxicities, such as hypertension, proteinuria, hypothyroidism, diarrhea, deep vein thromboses, fatigue, and surgical wound healing complications (Verheul and Pinedo, 2007). VEGF-blocking agents have also been associated with some rare, more serious, side effects including life-threatening thromboembolic events and severe bleeding complications (Chen and Cleck, 2009; Verheul and Pinedo, 2007). Antiangiogenic therapies need to be administered for months to years and may eventually prove useful in long-term adjuvant therapy for the prevention of recurrent disease, raising further concerns about long-term toxicities. Thus, drugs that can selectively target pathological host vasculature with minimal side effects are urgently needed.

Tumor endothelial marker 8 (TEM8) is a highly conserved single-pass cell-surface glycoprotein that was originally identified based on its overexpression in the endothelial cells (ECs) that line the tumor vasculature of human colorectal cancer (St. Croix et al., 2000). Although our understanding of its physiological function is limited, TEM8 has been found to bind to collagens and promote migration of ECs in vitro (Nanda et al., 2004; Werner et al., 2006). TEM8 was also identified as an anthrax toxin receptor (ANTXR1) (Bradley et al., 2001), and it shares 58% amino acid identity with CMG2, a second receptor for anthrax toxin protein (ANTXR2) (Scobie et al., 2003). TEM8 is upregulated on tumor vessels of various tumor types in both mice and humans (Carson-Walter et al., 2001; Fernando and Fletcher, 2009; Nanda et al., 2004), and in some tumors is also expressed by the tumor cells themselves (Carson-Walter et al., 2001; Jinnin et al., 2008; Yang et al., 2011b). TEM8 was unique among the original TEMs identified in that it could not be detected in the angiogenic corpus luteum of human ovaries (Nanda et al., 2004; St. Croix et al., 2000), and developmental angiogenesis and wound healing are unperturbed in *Tem8* knockout (KO) mice (Cullen et al., 2009). Indeed, aside from misaligned incisors, adult *Tem8* KO mice are overtly normal in appearance. However, murine B16 melanoma tumor growth was impaired in *Tem8* KO versus wild-type mice, demonstrating that host-derived TEM8 can promote tumor growth on an immunocompetent background (Cullen et al., 2009). Furthermore, previous studies have shown that a soluble TEM8-Fc trap, TEM8 vaccines, or sublethal doses of anthrax toxin can inhibit angiogenesis, slow tumor growth, and prolong survival (Duan et al., 2007; Felicetti et al., 2007; Liu et al., 2008; Rouleau et al., 2008; Ruan et al., 2009; Yang et al., 2010). Taken together, these studies suggest that TEM8 may be required for tumor angiogenesis but not physiological angiogenesis. Here we sought to develop anti-TEM8 antibodies that can block TEM8 function in an effort to selectively block pathological angiogenesis.

RESULTS

TEM8 Functions in Pathological but Not Physiological Angiogenesis

To obtain further evidence that TEM8 is selectively associated with pathological angiogenesis, we compared the *Tem8* expression pattern between tumor ECs and adult regenerating liver ECs. Following 70% partial hepatectomy, the remaining liver grows rapidly in a highly regulated angiogenesis-dependent process (Drixler et al., 2002; Seaman et al., 2007). In this model, quiescent ECs enter the cell cycle synchronously at around 24 hr postsurgery and cease proliferation about 72 hr later. To examine gene expression, we performed quantitative RT-PCR (QPCR) on ECs purified from tumor xenografts derived from DLD1, HCT116, or LS174T cells, or ECs isolated from quiescent resting liver (0 hr) or regenerating liver taken at various postsurgical time points (6, 18, 48, 72, or 96 hr). Although markers of proliferation, such as *Ki67*, protein regulator of cytokinesis 1 (*Prc1*), and thymidine kinase (*TK*) were highly induced in liver ECs by 48 hr postpartial hepatectomy, *Tem8* expression levels remained baseline in regenerating liver ECs. In contrast, *Tem8* was expressed 32- to 55-fold higher in each of the tumor EC fractions compared to resting liver ECs (Figure 1A). The peak expression levels of the cell-cycle genes in regenerating liver ECs were higher than that in tumor ECs, presumably because of the synchronous nature of the proliferating liver EC population.

To investigate whether *Tem8* is expressed by tumor-associated inflammatory cells, such as $CD11b^+$ myeloid cells or other bone marrow-derived cells that have been shown to promote tumor angiogenesis and may be involved in the refractoriness of tumors to VEGF inhibition (Du et al., 2008; Shojaei et al., 2007), we examined its expression in $CD45^+$ (pan hematopoietic), $CD11b^+$ (myeloid), and $CD105^+$ (endothelial) cells isolated from tumors. *Tem8* was highly expressed only in the endothelial fraction (Figure S1A available online). To determine potential tumor microenvironmental factors that induce TEM8 expression on tumor vasculature, we examined cultured human microvascular endothelial cells (HMECs) in response to several conditions. Neither coculture with tumor cells nor exposure to hypoxia induced TEM8 (Figures S1B and S1C). However, upon serum starvation, TEM8 levels steadily increased in these cells, which normally express low endogenous TEM8 levels, resulting in a 4-fold increase in *TEM8* mRNA (Figure 1B) and a 5-fold increase in TEM8 protein (Figure 1C) by day 10. In contrast, TEM8 levels remained low in cells maintained in complete medium, and the slight increase in TEM8 expression noted at later time points (Figures 1B and 1C) may have been due to rapid growth factor depletion caused by increasing cell numbers (Figure 1D, top). The increase in TEM8 expression upon growth factor starvation was not influenced by the amount of cell-cell contact, based on comparisons of sparse versus confluent cells wherein the cell numbers were held constant but the surface area was altered (data not shown). Importantly, TEM8 elevation in growth factor-starved cells could be inhibited by fibroblast growth factor (FGF), VEGF, or serum treatment, and the combination of all three resulted in the lowest TEM8 levels (Figures 1E and 1F; Figure S1D). Thus, TEM8 may be part of a compensatory angiogenic or survival pathway that is activated, at least in part, by insufficient local angiogenic growth factors.

Host-Derived TEM8 Promotes the Growth of Human Tumor Xenografts

To determine whether TEM8 could promote the growth of human tumor xenografts, we generated *Tem8* KO mice on an

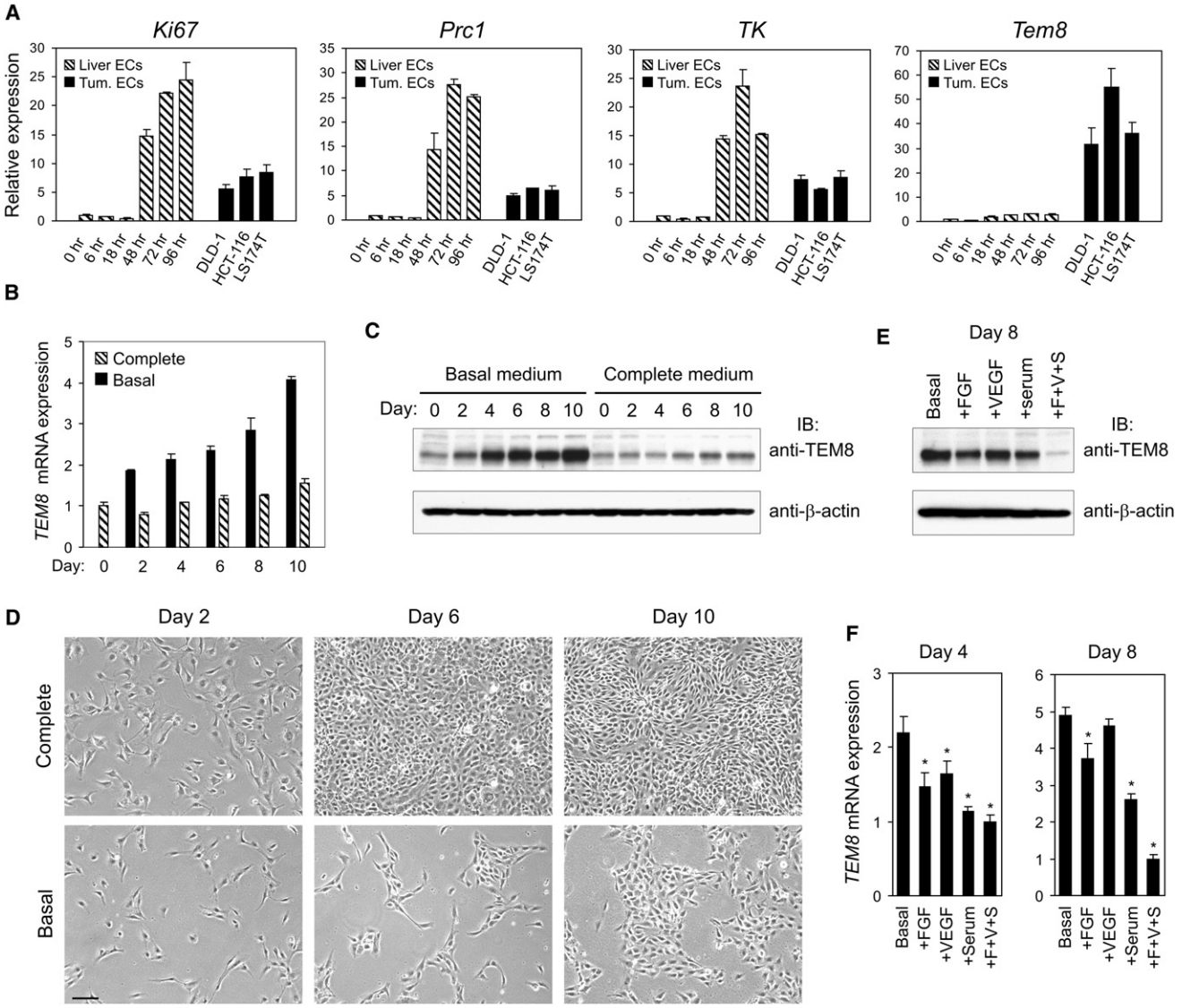

Figure 1. TEM8 Is Selectively Upregulated on Tumor Vasculature and Is Elevated in Cultured HMECs in Response to Growth Factor Deprivation

(A) QPCR was used to evaluate the expression of the indicated genes in ECs isolated from resting adult liver (0 hr), regenerating liver taken 6, 18, 48, 72, or 96 hr following 70% partial hepatectomy, or DLD1, HCT116, or LS174T colon cancer xenografts.

(B) *TEM8* mRNA levels over the course of 10 days in HMECs grown in endothelial basal medium (EBM-2) or in complete medium (EBM-2 supplemented with FGF [F], VEGF [V], and 5% fetal bovine serum [S]).

(C) TEM8 protein levels over the course of 10 days in HMECs grown in basal medium or in complete medium. The media are the same as in (B).

(D) The appearance of the cells used in (B) and (C) is shown. Note that HMECs became confluent by day 6 in complete medium but formed only small colonies by day 10 in basal medium. The media are the same as in (B). The scale bar represents 100 μm.

(E and F) Effect of supplementation of basal growth medium with FGF, VEGF, or serum alone or all three together on the expression of TEM8 protein (E) and mRNA (F) (*$p < 0.05$). Values in (A), (B), and (F) represent mean ± SD.

See also Figure S1.

immunocompromised athymic nude background. Tumor growth was inhibited in the *Tem8* KO mice compared to WT littermate controls when challenged with various tumor types including melanoma (UACC and LOX), breast (MDA-MB-231), lung (NCI-H460), and colon cancer (SW620, HCT116, and DLD1) (Figure 2). The MDA-MB-231 breast tumors were grown orthotopically in the mammary fat pad, whereas the melanoma and other tumor types were grown subcutaneously. Tumor growth was consistently slower in *Tem8* KO versus WT mice, and SW620 tumors required over 100 days to reach an average size of 800 mm^3, compared to only 35 days for WT littermates (Figure 2G). Thus, host-derived TEM8 functions to promote the subcutaneous and orthotopic growth of human tumor xenografts of diverse origin.

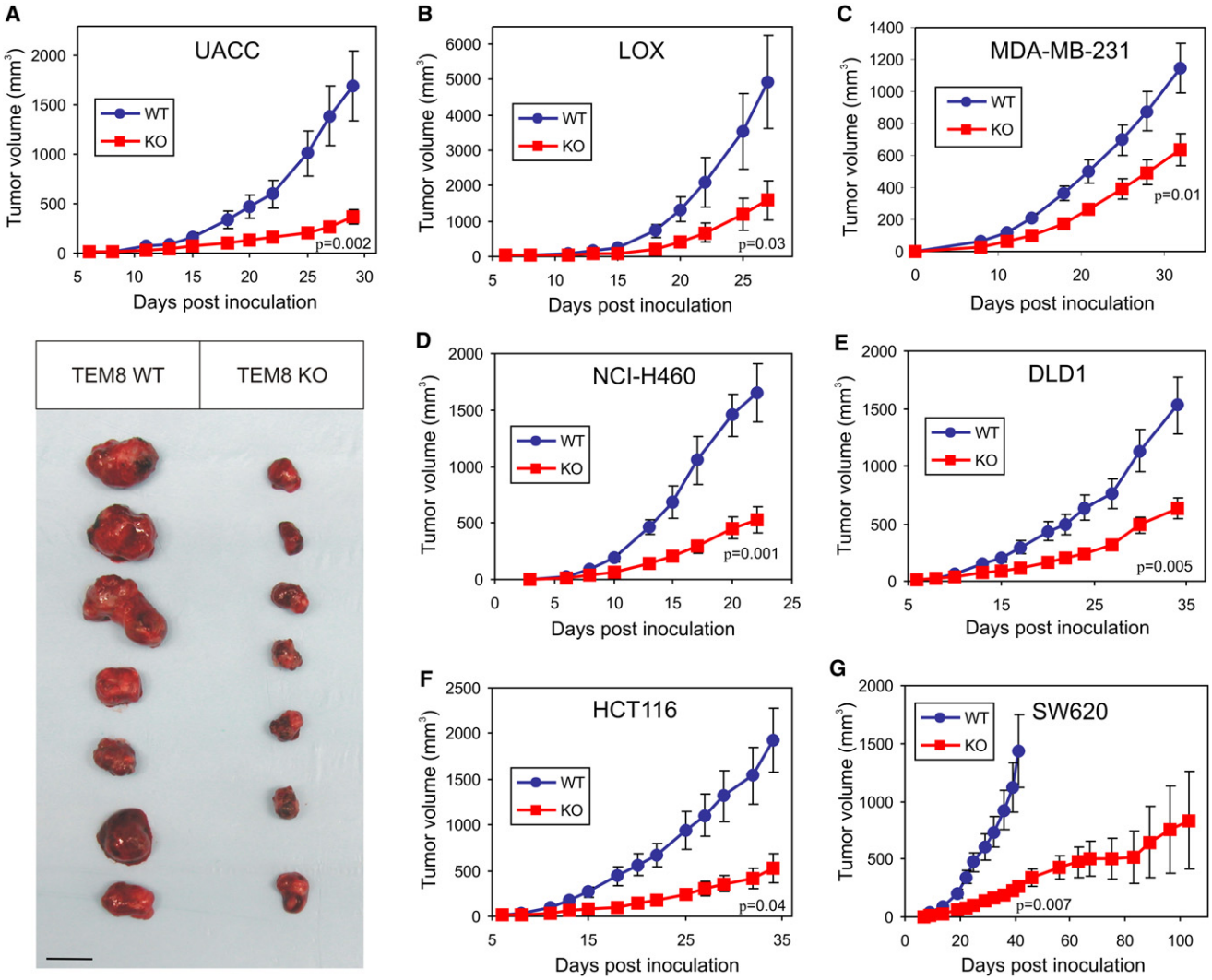

Figure 2. The Growth of Human Tumor Xenografts Is Impaired in *Tem8* KO Mice

Melanoma (A and B), breast (C), lung (D), and colon (E–G) cancer cell lines were injected into *Tem8* wild-type (blue) or knockout (red) mice and tumor volume was monitored over time. The physical appearance of the resected UACC tumors is shown in (A). p values were calculated from the final tumor measurement (A–F) or at day 41 (G), when the WT group reached its maximum size and had to be euthanized (Student's t test). n = 7–15 mice/group. Values represent mean ± SE. The scale bar represents 10 mm.

Development of Anti-TEM8 IgGs

Based on the functional importance of TEM8 in tumor growth promotion, we sought to develop therapeutic anti-TEM8 antibodies that could block TEM8 function in vivo. We had previously generated the SB series of anti-TEM8 antibodies (Nanda et al., 2004). However, these antibodies were murine derived and none of these could bind the predominant native form of TEM8 on the cell surface (Nanda et al., 2004; Yang et al., 2011b). To overcome these obstacles and circumvent potential difficulties associated with breaking tolerance, we developed another panel of fully human anti-TEM8 antibodies in vitro using antibody phage display. The selection strategy, which involved panning of Fab libraries on *Tem8*-transfected mammalian cells and purified recombinant mammalian-derived TEM8-ED (extracellular domain), resulted in the identification of five independent Fabs, L1, L2, L3, L5, and ID2. Each of the Fabs was found to react with both mouse and human TEM8 in an ELISA and on the surface of live TEM8-positive cells by immunofluorescence and flow cytometry (Figures S2A–S2C). Although the physiologic ligand(s) of TEM8 in vivo is unclear, the TEM8 extracellular region contains a single structural motif, that is, a von Willebrand factor type A (vWA) domain, where physiologic TEM8 ligand(s) is most likely to bind. vWA domains are found in many extracellular eukaryotic proteins including integrins, and are known to mediate adhesion to other proteins via metal-ion-dependent adhesion sites. We reasoned that the protective antigen (PA) subunit of anthrax toxin, which binds the exposed vWA domain of TEM8 in a metal-ion-dependent manner, may usurp the physiologic binding site of a natural ligand. Thus, we screened the Fabs for the ability to block FITC-labeled

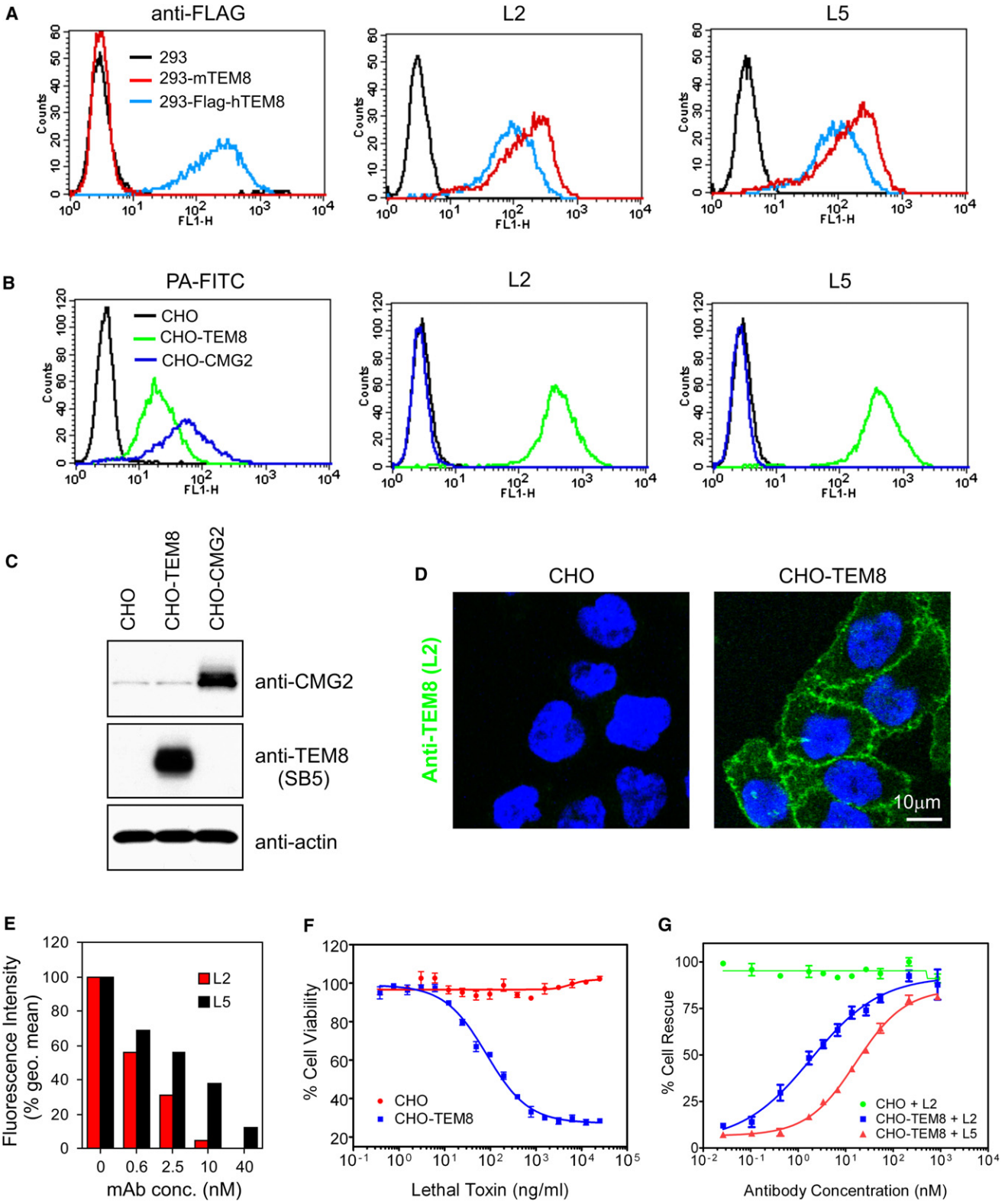

Figure 3. L2 and L5 IgGs React Selectively with TEM8 and Block Binding and Toxicity of Anthrax Toxin Proteins

(A) L2 and L5 antibodies were used for flow cytometry staining of 293 cells stably transfected with mouse *Tem8* (293-mTEM8) or a FLAG-tagged human *TEM8* (293-Flag-hTEM8).

(B) L2 and L5 were used for flow cytometry staining of CHO/PR230 (CHO) cells (an anthrax toxin receptor-deficient cell line) that had been stably transfected with human *TEM8* (CHO-TEM8) or human *CMG2* (CHO-CMG2). FITC-labeled protective antigen (PA-FITC), which binds both TEM8 and CMG2, was used as a positive control.

anthrax toxin PA binding to the surface of cells expressing TEM8. Each of the Fabs blocked FITC-PA binding in a dose-dependent manner (Figure S2D). Thus, we identified five human anti-TEM8 Fabs that were positive in all screens and that contained a unique variable domain.

Fabs have a relatively short half-life in vivo (several hours) compared to full IgGs (several days). To enhance their stability in vivo, two of the Fabs, L2 and L5, were selected for reformatting to full IgG. For preclinical testing in mice, the constant domains of mouse IgG2a (C_H1, C_H2, C_H3, and C_L) were fused to the human variable domains (V_H and V_L) in order to minimize immunogenicity, resulting in human-mouse chimeric antibodies. After reformatting, both L2 and L5 IgGs maintained their activity against TEM8 in the same screens used to test the Fabs, and were specific because they failed to react with mouse or human CMG2, the closest homolog of TEM8 (Figures 3A–3D and data not shown). Upon titration and comparison at nonsaturating concentrations, L2 bound TEM8-expressing cells with 7-fold higher affinity than L5 (EC_{50} 0.4 and 2.8 nM, respectively; see Figure S2E). Similarly, L2 was ~4-fold more potent at blocking the binding of FITC-labeled protective antigen and ~9-fold more potent at preventing cytotoxicity caused by anthrax lethal toxin (Figures 3E–3G).

Anti-TEM8 IgGs Inhibit Tumor Growth but Do Not Delay Wound Healing

We tested the L2 and L5 antibodies for their activity against UACC, HCT116, and DLD1 colon tumor xenografts in athymic nude mice. In these studies, mice were treated with L2 or L5 once tumors reached an average size of 50 mm^3. For each tumor type analyzed, a marked tumor growth inhibition was observed in each of the treated groups compared to vehicle (PBS) alone (Figures 4A–4E). The antitumor activity was comparable to that of anti-VEGFR2 antibodies (Figure 4C). When L2 and L5 were compared in a dose-escalation study to determine the amount of antibody required for optimal tumor growth inhibition, L2 showed superior activity. A partial growth inhibition was observed when mice were given 2 mg/kg of L2, whereas maximum growth inhibition was observed with 15 mg/kg (Figure 4E). L5, on the other hand, only showed partial growth inhibition at 15 mg/kg, similar to that observed in the 2 mg/kg L2 treatment group, and in each tumor study required 30–40 mg/kg to achieve its optimal biologic dose (OBD). Although L5 required a higher dose than L2 to achieve maximum efficacy, at their OBDs the two antibodies showed similar antitumor activity. Taken together, these studies demonstrate a marked in vivo antitumor activity of two independent anti-TEM8 antibodies. Because the full IgG of L2 appeared more potent than L5 both in vitro and in vivo, we focused on L2 for the remainder of our studies.

The aforementioned studies were conducted in immunocompromised mice. To determine whether L2 could suppress tumor growth in the presence of an intact immune system, we injected murine B16 melanoma cells into syngeneic C57BL/6 mice and began treating mice with L2 at a tumor size of 50 mm^3. The L2-treated group had a 60% reduction in tumor growth by the end of the study (Figure 4F). Midway through the therapeutic course, we also inflicted 6-mm-diameter wounds into each of the tumor-bearing mice to determine whether L2 treatment would interfere with wound healing. Wound closure rates were not significantly altered by L2 (Figure 4G), despite its clear antitumor activity in the same mice. Immunofluorescence staining for CD31 showed no alteration in the amount of vasculature present within the healing wound granulation tissue (Figure 4H). Matrigel-induced vascularization was also unaffected by L2 treatment (Figure 4I). Thus, L2 antibodies inhibited chronic pathological tumor growth while not interfering with normal healing processes dependent on physiological angiogenesis.

L2 Has No Detectable Toxicity

Two types of toxicology studies were conducted to determine how well the L2 anti-TEM8 antibody was tolerated. The first study involved dose escalation, wherein mice were administered 20, 50, or 100 mg/kg of L2 every other day for a total of three treatments and then analyzed 24 hr later. All serum chemistry and blood cell counts in the group treated with 100 mg/kg L2 were similar to that of the control group, and no dose-dependent alterations were observed (Table 1; data not shown). Treated mice consumed food and socialized similarly to control animals, and both body and organ weights were unchanged (Figures S3A and S3B). A comprehensive histopathologic analysis of 44 organs or tissues derived from 6 mice/group failed to reveal any abnormalities (data not shown). The second toxicology study involved treatment of mice with 20 mg/kg of L2 three times per week for up to 6 weeks, followed by an analysis of the same toxicology parameters. Again, no abnormalities were noted (Figure S3C; data not shown).

L2 Targets Tumor Vasculature In Vivo

To determine the specificity of L2 for TEM8 in vivo, we decided to treat tumor-bearing *Tem8* WT and KO mice with L2, reasoning that L2 should only have activity against tumors in *Tem8* WT mice if the tumor cells employed do not themselves express endogenous TEM8. TEM8 expression varied among cultured tumor cell lines, among which DLD1 tumor cells expressed undetectable TEM8 both in cell culture and following purification from established tumors in vivo (Figures S4A and S4B). Therefore, to test the specificity of the L2 antibody in vivo, *Tem8* WT and KO mice were challenged with DLD1 cells and treated with L2 or control IgG (Figure 5A). As expected, tumors grew more slowly in *Tem8* KO compared to *Tem8* WT mice treated with

(C) Western blot analysis was used to evaluate the expression of TEM8 and CMG2 in stably transfected CHO-TEM8 and CHO-CMG2 cells.
(D) L2 antibodies were used for cell-surface immunofluorescence labeling of CHO and CHO-TEM8 cells.
(E) The ability of L2 and L5 antibodies to block binding of PA-FITC to CHO-TEM8 cells was measured by flow cytometry.
(F) The viability of CHO and CHO-TEM8 cells was evaluated 48 hr posttreatment with lethal toxin.
(G) The ability of L2 and L5 antibodies to protect cells from toxicity following treatment with 1 μg of lethal toxin was evaluated. In this assay, the EC_{50} for L2 and L5 was 1.9 and 16.6 nM, respectively. Values in (F) and (G) represent mean ± SE.
See also Figure S2.

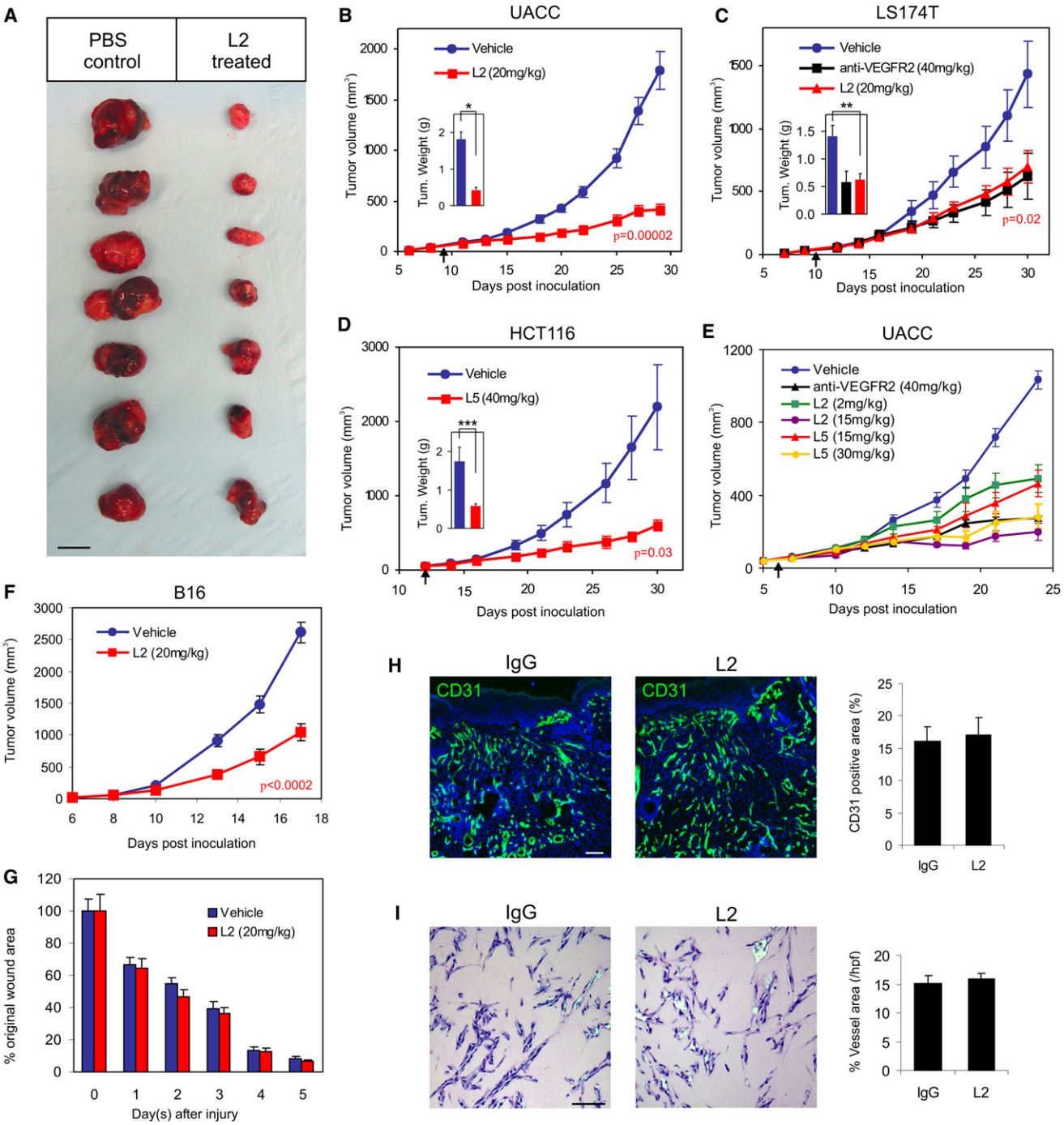

Figure 4. Anti-TEM8 Antibodies Inhibit Tumor Growth but Do Not Delay Wound Healing

(A–F) Melanoma (A, B, and E: UACC; F: B16) or colon cancer (C: LS174T; D: HCT116) tumor cells were inoculated subcutaneously into athymic nude (UACC, LS174T, HCT116) or C57BL/6 (B16) mice and tumor growth was monitored. Treatments with PBS (vehicle), anti-VEGFR2 antibodies, or anti-TEM8 antibodies (L2 or L5) were administered three times per week and were initiated when tumors reached a size of 50 mm^3 (arrows). A Student's t test was used to calculate p values between the vehicle and L2 treatment groups at the final tumor measurement. Tumors were excised at the end of the study to calculate final tumor weights (insets in B–D). *p = 0.00005, **p = 0.002, ***p = 0.02.

(A) The physical appearance of the UACC melanoma tumors at the end of the study following surgical excision. The scale bar represents 10 mm.

(B) L2 inhibition of UACC melanoma tumor growth.

(C) L2 and DC101 (anti-VEGFR2) inhibition of LS174T tumor growth.

(D) L5 inhibition of HCT116 tumor growth.

(E) L2 and L5 dose-dependent inhibition of UACC tumor growth.

(F) L2 inhibition of B16 melanoma tumor growth.

control IgG. When the L2 antibody was administered to *Tem8* WT mice, tumor growth was inhibited relative to the IgG control group but was indistinguishable from that in the *Tem8* KO group. Importantly, L2 treatment of *Tem8* KO tumor-bearing mice did not result in any further tumor growth inhibition. Taken together, these results indicate that TEM8 is the sole target of L2 in vivo, and supports the hypothesis that L2 is a function-blocking monoclonal antibody.

The previously described expression of TEM8 in tumor endothelium (Fernando and Fletcher, 2009; Nanda et al., 2004; St. Croix et al., 2000) suggests that the target tissue of L2 in vivo may be the tumor-associated vasculature. To assess this, we performed CD31 vessel staining of the human DLD1 colon cancer xenografts and found a reduced number of vessels in tumors derived from *Tem8* KO or L2-treated mice (Figure 5B). Quantification of the number of CD31-positive ECs in tumors using flow cytometry revealed significantly lower EC numbers following both pharmacologic and genetic ablation of TEM8 (Figure 5C). We reasoned that TEM8 may promote proliferation of tumor ECs, based on previous studies that showed a role for CMG2 in promoting endothelial proliferation (Reeves et al., 2010). However, endothelial proliferation in DLD1 tumors was not altered in response to L2 treatment (Figure S4C), although the number of apoptotic ECs was significantly increased ($p < 0.02$; Figure S4D).

To further assess the specificity of L2 in vivo, L2 was labeled with FITC and then intravenously injected into DLD1 tumor-bearing mice. Immunofluorescence analysis revealed localization of TEM8 selectively in tumor-associated vasculature but not in any of the normal control tissues analyzed including brain, heart, intestine, liver, muscle, spleen, and stomach (Figure 5D). Some tumor-associated perivascular stromal cells, including pericytes based on their adjacent proximity to endothelium, were also positive. However, stromal cell staining was confined to the tumor region in *Tem8* WT mice and was absent from the tumors in *Tem8* KO mice, confirming the specificity of antibody staining (Figure 5E).

L2 Can Elicit NK-Mediated and Complement-Mediated Cytotoxicity

We reasoned that the antitumor activity of L2 in vivo may involve multiple mechanisms, and that antibody-dependent cellular cytotoxicity (ADCC) and/or complement-dependent cytotoxicity (CDC) could contribute to this activity. To determine whether TEM8 could potentially function as a target of ADCC, we mixed effector natural killer cells with TEM8-expressing 293 target cells at various ratios and found that L2, but not control IgG, was able to elicit cytotoxicity that was dependent on both the antibody and effector cell concentration (Figures 5F and 5G). Similarly, L2 elicited CDC in both an antibody- and complement-dependent manner (Figures 5H and 5I). Although these in vitro studies support a role for ADCC and CDC, further work is required to determine whether these mechanisms contribute to the antitumor activity of L2 in vivo.

Table 1. Selected Toxicological Results and Organ Weights

	Control	100 mg/kg L2 Anti-TEM8
Selected Parameters		
White blood cells (K/μl)	5.9 ± 2.5	6.3 ± 2.4
Red blood cells (M/μl)	9.5 ± 0.4	9.6 ± 0.4
Albumin (g/dl)	4.0 ± 0.4	3.9 ± 0.1
Alanine aminotransferase (U/l)	52.7 ± 10.1	51.9 ± 27.4
Total bilirubin (mg/dl)	≤0.2	≤0.2
Creatine (mg/dl)	≤0.2	≤0.2
Hemoglobin (g/dl)	13.9 ± 0.6	13.9 ± 0.4
Total protein (g/dl)	5.6 ± 0.2	5.7 ± 0.4
Blood urea nitrogen (mg/dl)	19.7 ± 2.0	17.5 ± 3.4
Selected Organ Weights (mg)		
Brain	462 ± 19	465 ± 15
Heart	137 ± 15	155 ± 21
Kidney	312 ± 58	308 ± 63
Liver	1,173 ± 180	1,152 ± 271
Lung	153 ± 20	168 ± 34
Spleen	80 ± 13	83 ± 15

Represented toxicological data and organ weights from mice (n = 6/group) dosed i.p. every second day with saline (control) or 100 mg/kg anti-TEM8 mAb. Values are mean ± SD.
See also Figure S3.

L2 Potentiates Tumoricidal Responses

The delayed tumor growth in *Tem8* KO mice and the encouraging antitumor activity of L2 against relatively small established 50 mm^3 tumors prompted us to explore the activity of L2 against larger tumors. Importantly, even tumors that were 200 mm^3 in size prior to L2 treatment showed a significant response to the antibody such that when the control tumors reached an average size of 2,000 mm^3, treated tumors had an average size of 1,288 mm^3 (Figure 6A). However, because the L2-mediated growth inhibition was less effective against relatively large (200 mm^3) preestablished tumors compared to small (50 mm^3) tumors (compare L2-treated group in Figure 6A with that in Figure 4B), we determined whether the combination of L2 with other types of anticancer agents would result in enhanced antitumor efficacy. When L2 treatment was combined with the anti-VEGFR2 antibody DC101, which prevents VEGF from binding VEGFR2, L2 significantly enhanced the activity of DC101 against UACC melanoma ($p < 0.05$; Figure 6A). Furthermore, the combination of L2 with DMXAA (ASA404), a vascular targeting agent that has shown promising activity in early clinical trials against lung cancer (Baguley and McKeage, 2010), proved highly

(G) Wound closure rates following treatment with L2 or vehicle (PBS) alone. In this experiment, wounds were generated in the same tumor-bearing mice as shown in (F).
(H) CD31 immunofluorescence staining of granulation tissue vasculature in control and L2-treated groups. Control mice received nonspecific IgG in this experiment (n = 6 wounds/group).
(I) Matrigel plug vascularization was assessed following treatment with nonspecific IgG or L2 anti-TEM8 antibodies. Vessel areas were calculated from six plugs per group. Values in (B)–(I) represent mean ± SE. The scale bars (H and I) represent 100 μm.

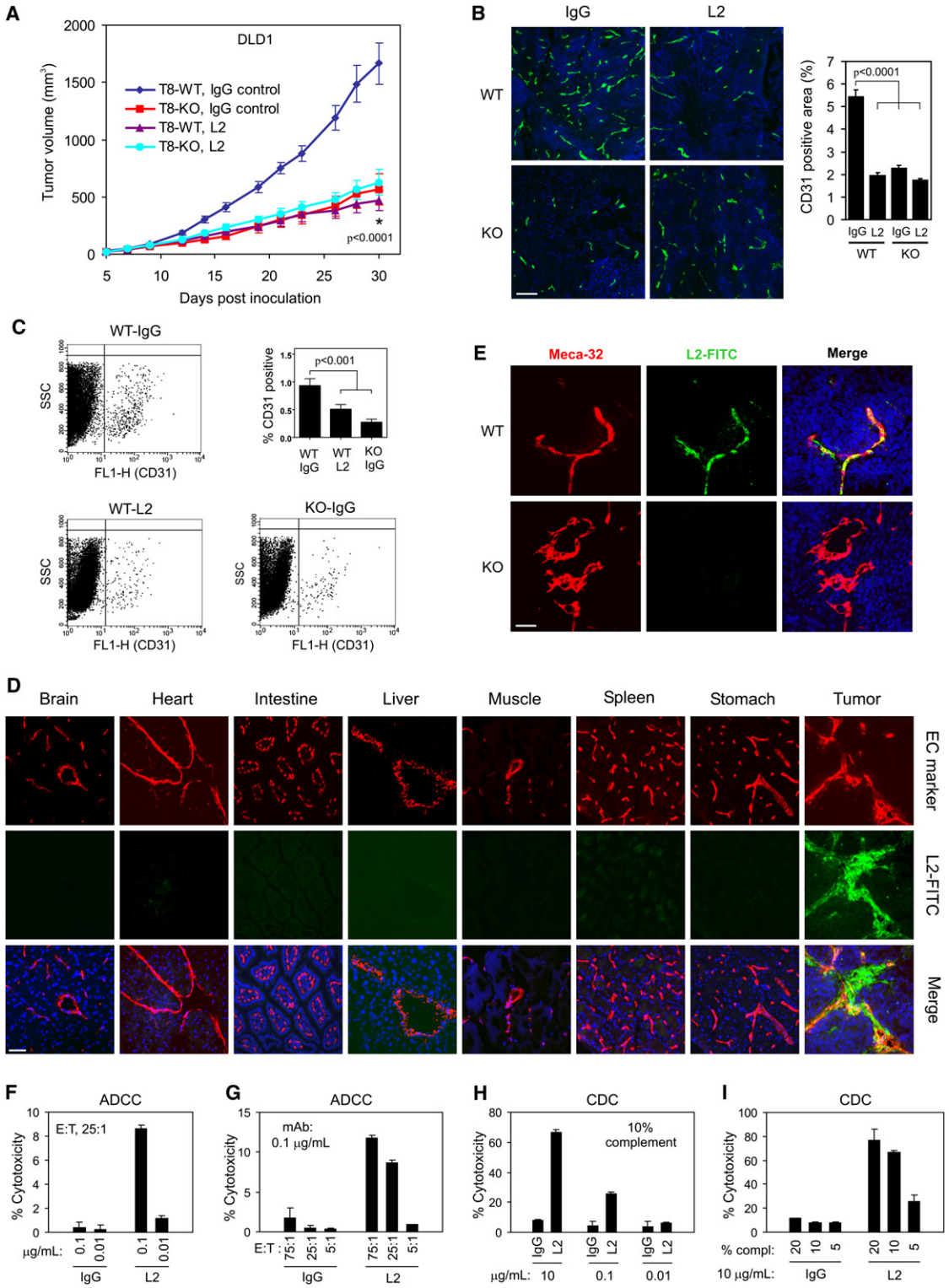

Figure 5. L2 Targets Tumor Vasculature In Vivo and Engages ADCC and CDC In Vitro

(A) Nonspecific antibodies (IgG control) or L2 anti-TEM8 antibodies were administered to *Tem8* wild-type (T8-WT) or *Tem8* knockout (T8-KO) mice at 20 mg/kg mice three times per week beginning 1 day post-subcutaneous inoculation of TEM8-negative DLD1 tumor cells. At day 30 (asterisk), the tumors in the T8-WT + IgG control group were significantly larger than those in each of the other three groups ($p < 0.0001$), but there was no difference in tumor size between the T8-KO + IgG, T8-WT + L2, and T8-KO + L2 groups (one-way ANOVA with Bonferroni posttest) ($n = 12$ mice/group).

(B) Immunofluorescence vessel staining of *Tem8* WT and KO mice following treatment with L2 or IgG. Right: quantification of CD31-positive vessel area. $p < 0.0001$ between each of the groups and the IgG WT control group (one-way ANOVA). The scale bar represents 200 μm.

effective against NCI-H460 lung cancer xenografts (Figure 6B). Both L2 and DMXAA significantly delayed tumor growth, but the combination was even more efficacious than either treatment alone ($p < 0.001$; DMXAA + L2 versus DMXAA alone). Finally, when L2 was combined with 5-fluorouracil (5FU) and irinotecan (IRT), chemotherapeutic agents that are currently used to treat patients with colorectal cancer, L2 significantly enhanced their efficacy against HCT116 tumors ($p < 0.0001$, 5FU + L2 versus 5FU; $p < 0.02$, IRT + L2 versus IRT; Figures 6C and 6D). L2 also enhanced the efficacy of irinotecan against SW620 ($p < 0.02$, IRT + L2 versus IRT; Figure 6E), another colon cancer tumor model, demonstrating the generality of this response. Combination of L2 with IRT was highly efficacious, such that tumors in 5 of 11 mice in the HCT116 study and 4 of 11 mice in the SW620 study had completely regressed by 100 days postinoculation, and these mice remained tumor free for the duration of the study, an additional 7 months (Figures 6D and 6E). No complete tumor responses were observed in any of the monotherapy treatment arms. To further assess the inhibitory activity of L2 + IRT following long-term therapy, treatment was discontinued after 100 days, which resulted in rapid expansion of the remaining tumors that had not completely regressed. Analysis of body weights, food consumption, serum chemistry, and hematological profiles in these combination drug trials failed to reveal a change in toxicity caused by the addition of L2 to the chemotherapeutic agent (Figure 6F; Table S1). Taken together, these studies demonstrate that L2 treatment can enhance the antitumor responses of a wide variety of anticancer agents without added toxicity.

L2 Binds Human Tumor Vasculature

To examine the specificity of L2 binding in human tumors, in situ immunofluorescence staining with L2 was performed on colorectal tumors or adjacent normal colonic mucosa derived from six cases of late-stage colorectal cancer, four of which were patient matched. Although staining was undetectable in all cases of normal colonic mucosa, in each of the tumor samples L2-FITC strongly labeled the tumor stroma, including von Willebrand factor (vWF)-positive ECs as well as some perivascular stromal cells that, based on morphology, appeared to include pericytes and possibly fibroblasts (Figure 7). Although the intensity of stromal staining was variable in different regions of the tumor, the staining was considered specific because it was completely blocked by the addition of unlabeled L2 but not isotype-matched control IgG. Thus, in tumors derived from both patients and mouse xenografts, TEM8 is found in tumor-associated vasculature and tumor-associated perivascular stromal cells.

DISCUSSION

These studies demonstrate that TEM8 is critical for promoting pathological angiogenesis evoked by a variety of tumor types, and that antibody-mediated targeting of TEM8 provides a rational strategy for combating cancer. Most angiogenesis regulators that have been discovered to date cannot distinguish physiological and pathological angiogenesis. In immunocompetent mice, L2 inhibited tumor growth but had no effect on wound healing in the same mice, consistent with earlier studies demonstrating no difference in wound healing between *Tem8* WT and KO mice (Cullen et al., 2009). TEM8 was also dispensable for developmental angiogenesis and normal physiological angiogenesis of the corpus luteum (Cullen et al., 2009; Nanda et al., 2004; St. Croix et al., 2000). A function for TEM8 in these normal physiological processes could potentially be masked through compensation by another molecule. However, CMG2 is the only other protein that shares significant amino acid identity with TEM8 and, aside from misaligned incisors, *Cmg2*/*Tem8* double-mutant mice, like *Tem8* KO mice, appear to develop normally (Liu et al., 2009). These results support the conclusion that physiological and pathological angiogenesis are distinct and that antibody-mediated targeting of TEM8 can selectively inhibit pathological tumor growth while sparing normal healing processes that also require vascularization.

Based on our results, we propose that TEM8 overexpression in tumor vasculature may be caused, at least in part, by local decreases in the availability of stromal growth factors, such as VEGF and FGF. At first, this might seem counterintuitive, given the overall proangiogenic nature of tumors. However, blood flow through the tortuous vessels in tumors is known to be slow, erratic, and often static, which could contribute to the rapid local depletion of angiogenic growth factors. Tumor ECs may also have to compete for growth factors with tumor cells that often express VEGF and/or FGF receptors themselves and can sometimes utilize angiogenic growth factors for their own growth (Dallas et al., 2007; Masood et al., 2001). Finally, hypoxia, a well-known inducer of VEGF gene transcription, may also lead to overexpression of the high-affinity VEGFR1

(C) Flow cytometry staining of dispersed tumor tissues was used to determine the percentage of CD31-positive cells in L2-treated tumors from *Tem8* WT mice (WT-L2), IgG-treated tumors from *Tem8* KO mice (KO-IgG), and IgG-treated tumors from *Tem8* wild-type mice (WT-IgG). The dot plots show representative data for each of the groups, and the bar graph displays the average percentage of CD31-positive cells (n = 6/group). Both the WT-L2 and KO-IgG groups had significantly fewer cells than the WT-IgG group, as determined by a one-way ANOVA.
(D) L2 localization in vivo was assessed by immunofluorescence staining of various tissues following i.v. injection of FITC-labeled L2 into DLD1 tumor-bearing mice. An overlay of the L2 image (green) with the endothelial marker image (Meca-32 or CD31, red) was used to assess colocalization with vasculature (yellow, merge). The scale bar represents 50 μm.
(E) The specificity of L2-FITC for TEM8 in vivo was assessed by comparing the staining of tumor stroma from *Tem8* wild-type and *Tem8* knockout mice. The scale bar represents 50 μm.
(F) NK-mediated toxicity against TEM8-expressing target cells was measured in the presence of L2 or control IgG. The effector:target (E:T) cell ratio in this experiment was 25:1.
(G) The impact of increasing E:T cell ratios on L2-mediated ADCC was evaluated.
(H) Complement-dependent cytotoxicity was assessed with varying amounts of L2 or control IgG.
(I) To evaluate complement dependency, variable amounts of complement were added to the CDC assay. Values in (A)–(C) and (F)–(I) represent mean ± SE.
See also Figure S4.

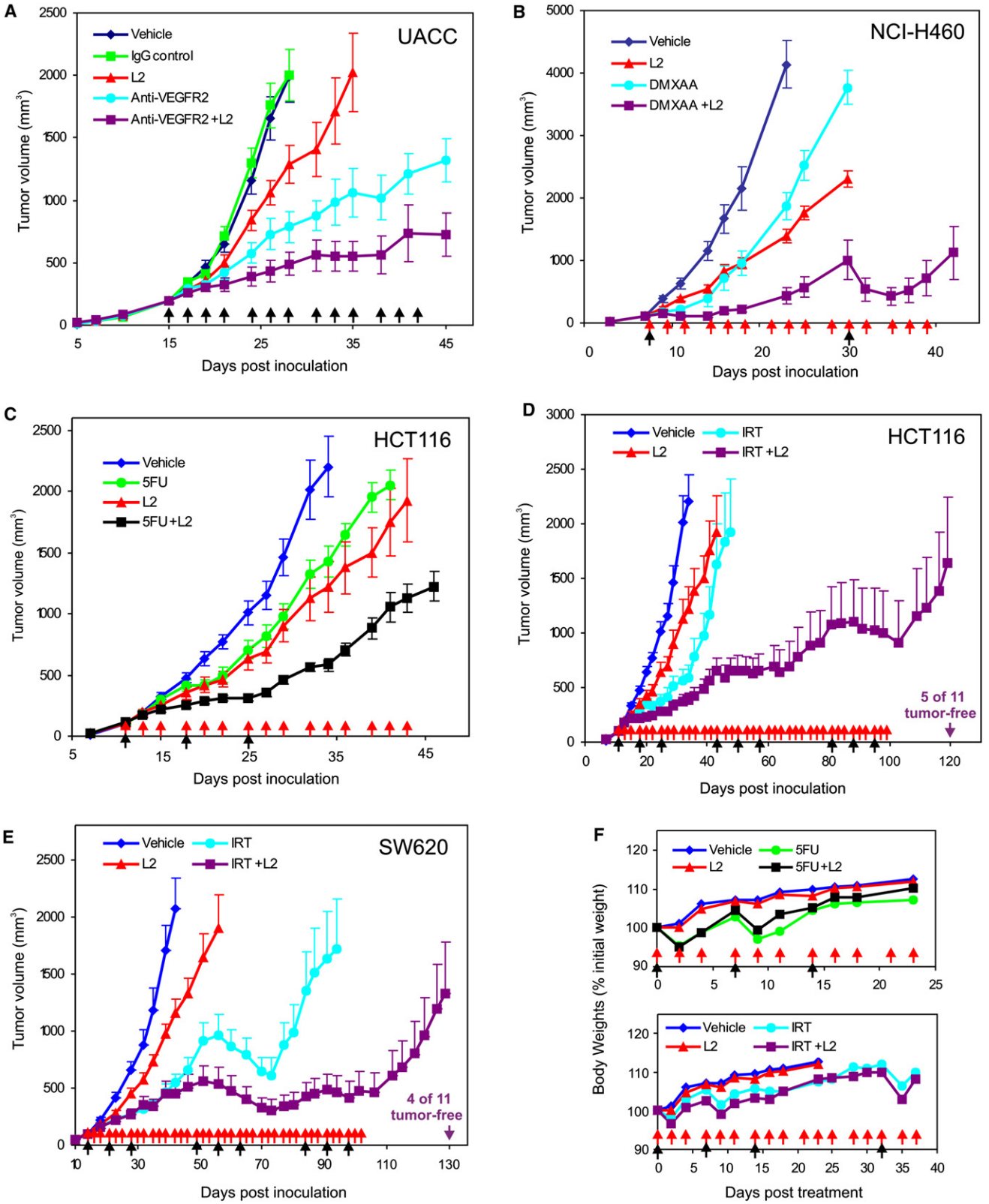

Figure 6. L2 Anti-TEM8 Antibodies Augment the Efficacy of Various Classes of Anticancer Agents

(A) UACC tumor growth was compared following treatment with vehicle (PBS), nonspecific mouse IgG (20 mg/kg), L2 anti-TEM8 (20 mg/kg), anti-VEGFR2 (40 mg/kg), or a combination of L2 (20 mg/kg) and anti-VEGFR2 (40 mg/kg). Treatments were administered three times per week (arrows) beginning 15 days post-tumor cell inoculation when tumors reached a size of 200 mm^3.

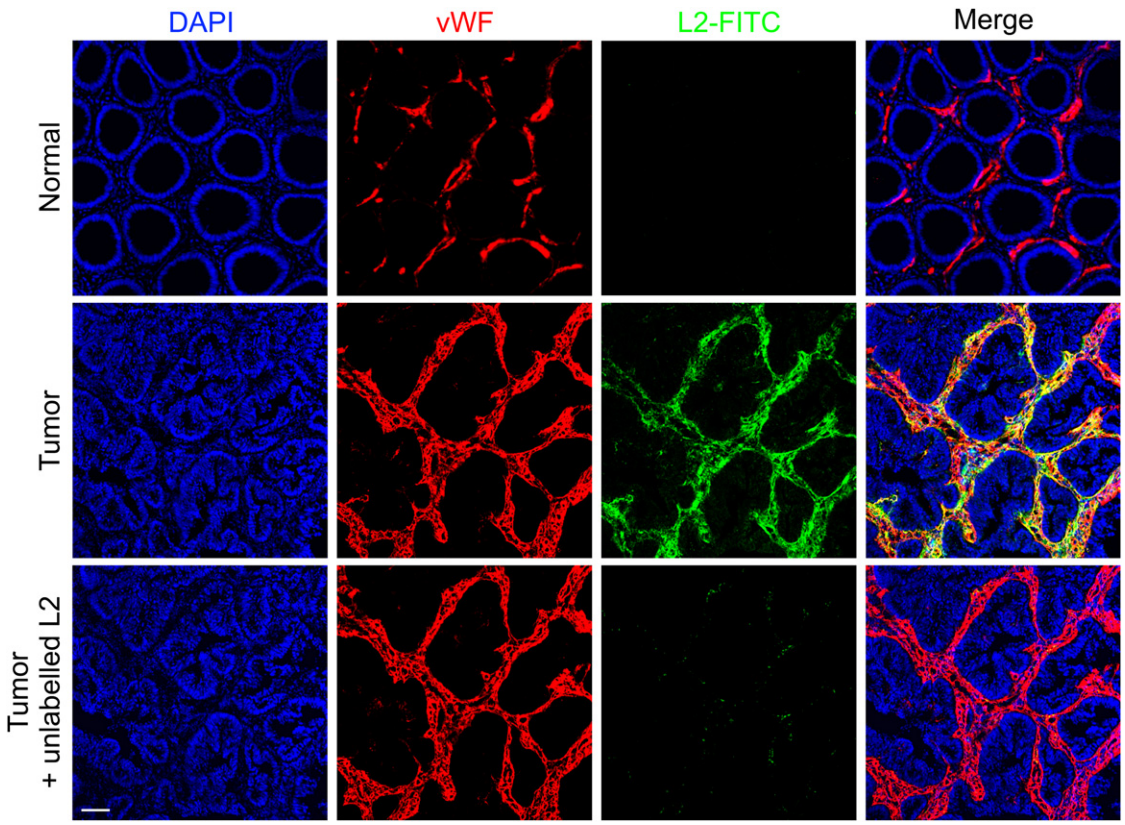

Figure 7. L2 Anti-TEM8 Antibodies Bind to the Vasculature of Human Colorectal Cancer

FITC-conjugated L2 (green) was used for immunofluorescence labeling of human colorectal tumors and normal colonic mucosa. The vasculature was costained with antibodies against von Willebrand factor (red), a pan endothelial marker, and overlapping immunofluorescence is shown in the merged image (yellow). The normal and tumor samples shown were patient-matched and processed in parallel. To prevent nonspecific binding, immunofluorescence staining was performed in the presence of a 50-fold excess of isotype-matched (human-mouse chimeric) control IgG that was generated against a foreign antigen (cyclosporine A). The staining was abolished by blocking the samples with unlabeled L2 (bottom) prior to adding L2-FITC. The middle and bottom panels were taken from serial sections. The scale bar represents 100 μm.

(Gerber et al., 1997) or its soluble splice variant sVEGFR1 that can act as decoy receptors, limiting VEGF bioavailability (Lamszus et al., 2003; Yamaguchi et al., 2007; Yang et al., 2011a). Elevated TEM8 expression in tumor ECs in response to growth factor deprivation and possibly other unidentified microenvironmental stressors may be part of a survival pathway that helps

(B) NCI-H460 tumor growth was compared following treatment with vehicle, L2 anti-TEM8, DMXAA, or a combination of L2 and DMXAA beginning 15 days post-tumor inoculation when tumors reached an average size of 100 mm^3. In this experiment, L2 (20 mg/kg) was administered three times per week (red arrows) for the duration of the study, whereas DMXAA was administered at a high dose of 25 mg/kg (black arrows), followed by 5 mg/kg/day the following 2 days.
(C) HCT116 tumor growth was compared following treatment with vehicle, L2 anti-TEM8 (20 mg/kg), 5-fluorouracil (100 mg/kg), or a combination of L2 and 5FU beginning 11 days post-tumor inoculation when tumors reached an average size of 100 mm^3. In this experiment, L2 was administered three times per week (red arrows), whereas 5FU was administered once a week for 3 weeks (black arrows).
(D) HCT116 tumor growth was compared following treatment with vehicle, L2 anti-TEM8 (20 mg/kg), irinotecan (80 mg/kg), or a combination of L2 and irinotecan beginning 11 days post-tumor inoculation when tumors reached a size of 100 mm^3. In this experiment, L2 was administered three times per week (red arrows) until 100 days postinoculation. To maximize efficacy without excessive toxicity and mimic the clinical situation, IRT was administered in three cycles (where 1 cycle = 1 treatment per week for 3 weeks; black arrows) that were separated by a 2 week rest period to allow recovery. The HCT116 tumor studies in (C) and (D) were conducted simultaneously and contain the same vehicle and L2 groups, which were duplicated for ease of comparison.
(E) SW620 tumor growth was compared following treatment with vehicle, L2 anti-TEM8 (20 mg/kg), irinotecan (80 mg/kg), or a combination of L2 and irinotecan beginning 14 days post-tumor inoculation when tumors reached a size of 100 mm^3. The treatments in this study were the same as those described for HCT116 above. IRT caused tumor regression in many of the treated mice. A decrease in tumor size caused by IRT is readily observed in both IRT arms (IRT and IRT + L2) during the second cycle of IRT treatment. During the subsequent 2 week rest period the tumors rapidly rebounded. Following the last cycle of IRT, many of the tumors in the combination group (IRT + L2) regressed again, whereas the larger tumors in the control group did not respond. For ease of comparison, only half of the error bars are shown in (D) and (E).
(F) Body weights in HCT116 tumor-bearing mice from the 5FU study (upper, corresponding to C) or the irinotecan study (lower, corresponding to D) were monitored from the start of therapy until the tumors in the control groups reached their maximum allowable size and mice had to be euthanized. Data represent mean values. The SD ranged from 2% to 8% and error bars are omitted for clarity. The apparent reduction in mean body weight observed following 5-fluorouracil and irinotecan treatments (black arrows) were nonsignificant and were not altered by L2 treatment (red arrows). Values in (A)–(E) represent mean ± SE. See also Figure S5.

ECs cope during suboptimal growth conditions. *Tem8* KO mice provide a valuable tool for assessing the role of TEM8 in pathological angiogenesis. For most pharmacological angiogenesis inhibitors, it is difficult to find animal models completely lacking the drug target because the target proteins are usually required for developmental angiogenesis, and temporally induced deletion of a conditional ''floxed'' target gene in adult mice using cre-lox technology is often incomplete. Importantly, by treating *Tem8* WT or KO mice with L2 anti-TEM8 antibody, we could verify that TEM8 is the target of this antibody in vivo, and that L2 treatment inhibits tumor growth to a level similar to complete genetic ablation. Further evidence for antibody specificity was obtained using FITC-labeled L2 that selectively reacted with the tumor vessels in *Tem8* WT but not KO mice.

Multiple mechanisms could potentially contribute to the antitumor activity of L2 in vivo, but so far the evidence suggests that the antibodies work primarily by blocking TEM8 function and that ADCC and CDC may play a more limited role. The extent of tumor growth delay observed in *Tem8* KO mice was found to vary depending on the tumor type employed, but the same tumor-type-dependent responses were observed following L2 blockade. For example, UACC tumors consistently displayed the most pronounced growth delay in *Tem8* KO versus WT mice, and were also the most responsive to L2. Indeed, the tumor growth patterns observed in *Tem8* KO mice were found to be indistinguishable from those observed in the L2-treated *Tem8* WT mice, provided that L2 treatment began immediately following tumor cell inoculation (for example, see Figure 5A). It is currently unclear why some tumor types rely more on host-derived TEM8 than others, but the degree of TEM8 dependence does not appear to correlate with the tumor cells' ability to evoke TEM8 expression in nearby tumor-associated ECs. For example, in *Tem8* WT mice, tumor ECs isolated from LLC tumors expressed four times more *Tem8* than those isolated from B16 tumors, yet comparisons of tumor growth in *Tem8* WT and KO mice revealed that B16 tumors are more dependent on host-derived TEM8 than LLC cells (Cullen et al., 2009). We expect that if ADCC and CDC were the major mechanisms governing tumor responses in vivo, then tumor responsiveness would have correlated with TEM8 expression levels in tumor ECs, because ADCC and CDC both depend on target antigen expression levels. Therefore, further studies are required to establish whether ADCC and CDC contribute significantly to L2's activity in vivo. Nevertheless, affinity maturation of the variable domain and modifications to the Fc domain that enhance ADCC and CDC activity (Natsume et al., 2009) could lead to further enhancement of antitumor efficacy.

Although anti-TEM8 antibodies inhibited tumor growth as a monotherapy, based on our results we predict that TEM8 antibodies may be most useful in combination with other agents. TEM8 antibodies were completely nontoxic and displayed efficacy when combined with various classes of anticancer agents. That anti-TEM8 antibodies augment the activity of VEGFR2-neutralizing antibodies suggests that signaling pathways involving TEM8 may be responsible, at least in part, for angiogenesis that persists following VEGF/VEGFR2 inhibition. Although human-mouse chimeric antibodies were employed in the preclinical studies described here, reengineering of the Fc domain can be used to make the IgG fully human for future clinical development.

In summary, we report the development of anti-TEM8 antibodies that retard tumor growth by inhibiting tumor angiogenesis. Anti-TEM8 antibodies were nontoxic and maintained efficacy in combination with various classes of anticancer agents. Thus, anti-TEM8 antibodies provide a rationally designed tool for selectively inhibiting pathological angiogenesis with important ramifications for the management of angiogenesis-dependent diseases.

EXPERIMENTAL PROCEDURES

Antibody Production and Purification

In vitro selection of the Morphosys HuCAL Gold phage library involved two rounds of sequential panning on biotinylated, purified recombinant TEM8(ED)-Fc fusion proteins, prepared as described in Supplemental Experimental Procedures, and one round of panning on HEK293 cells transfected with human *TEM8* (293/Flag-hTEM8). DNA inserts for the Fab heavy and light chains were subcloned and expressed, and bivalent Fabs were evaluated for TEM8 binding by ELISA (see Supplemental Experimental Procedures). Two of the TEM8-binding clones (L2 and L5) were reformatted to generate mouse-human chimeric full IgGs. Anti-TEM8 antibodies were collected from HEK293T culture supernatants and purified by protein A and size exclusion chromatography.

Western Blotting

Western blotting was performed using antibodies against TEM8 (clone SB5; Nanda et al., 2004), CMG2 (a kind gift from Stephen Leppla), actin (Chemicon), or HIF-1α (Novus Biologicals) as previously described (Cullen et al., 2011).

Animal and Tumor Studies

To derive *Tem8* KO mice on an immunodeficient background, *Tem8* KO mice on a C57BL/6 background (Cullen et al., 2009) were crossed with athymic NCr-nu/nu mice, and only *Tem8* WT and KO littermates derived from *Tem8* heterozygous intercrosses were used for comparison. Tumors were measured with a caliper, and tumor volumes were calculated using the formula length $\times$ width^2 $\times$ 0.5 and presented as the mean $\pm$ SE. All animal studies were carried out in accordance with protocols approved by the NCI Animal Care and Use Committee.

Immunofluorescence

For in vivo target identification, FITC-labeled L2 was coinjected with nonspecific mouse IgG intraperitoneally into DLD1 tumor-bearing *Tem8* WT and KO mice. Frozen sections were labeled with rat anti-PV-1 (Meca-32) or rat anti-CD31 (BD Pharmingen) antibodies. For immunofluorescence staining of human normal colonic mucosa or colorectal cancer, frozen tissue sections were blocked with nonspecific mouse-human chimeric IgG antibodies (mouse Fc/human Fab) generated against cyclosporine A and detected with L2-labeled FITC. The anonymized human colon tissue samples were obtained from the Cooperative Human Tissue Network with approval from the NIH Office of Human Subject Research. Further details regarding the immunofluorescence staining can be found in Supplemental Experimental Procedures.

Statistical Analysis

A Student's t test was used to calculate differences in tumor volumes or weights between two groups (for example, *Tem8* WT and KO mice) at the time when the WT (or control) group reached its maximum size and had to be euthanized. For comparisons between multiple tumor groups, a one-way ANOVA was used with a Bonferroni posttest. A one-way ANOVA was used for comparisons of microvascular densities and the fraction of CD31-positive cells by flow cytometry. p values < 0.05 were considered significant.

SUPPLEMENTAL INFORMATION

Supplemental Information includes four figures, one table, and Supplemental Experimental Procedures and can be found with this article online at doi:10.1016/j.ccr.2012.01.004.

ACKNOWLEDGMENTS

We thank Drs. Bert Vogelstein, Terry Van Dyke, Lino Tessarollo, and Isaiah J. Fidler for helpful suggestions. We thank Rou-Fun Kwong for help with the initial selection and characterization of anti-TEM8 antibodies. We thank Dr. Stephen H. Leppla, National Institute of Allergy and Infectious Diseases, NIH, for the CHO, CHO/TEM8, and CHO/CMG2 cells, recombinant PA, and lethal factor, and Dr. Arthur E. Frankel for the AF334 hybridoma. This work was supported in part by a Cooperative Research and Development Agreement between the Novartis Institutes for BioMedical Research and the intramural research program of the NCI, NIH, Department of Health and Social Services (DHSS), and with federal funds from the NCI under contract no. HHSN261200800001E. The content of this publication does not necessarily reflect the views or policies of the DHSS nor does mention of trade names, commercial products, or organizations imply endorsement by the U.S. government.

Received: May 12, 2011
Revised: September 19, 2011
Accepted: January 5, 2012
Published: February 13, 2012

REFERENCES

Baguley, B.C., and McKeage, M.J. (2010). ASA404: a tumor vascular-disrupting agent with broad potential for cancer therapy. Future Oncol. *6*, 1537–1543.

Bradley, K.A., Mogridge, J., Mourez, M., Collier, R.J., and Young, J.A. (2001). Identification of the cellular receptor for anthrax toxin. Nature *414*, 225–229.

Brastianos, P.K., and Batchelor, T.T. (2010). Vascular endothelial growth factor inhibitors in malignant gliomas. Target. Oncol. *5*, 167–174.

Carson-Walter, E.B., Watkins, D.N., Nanda, A., Vogelstein, B., Kinzler, K.W., and St. Croix, B. (2001). Cell surface tumor endothelial markers are conserved in mice and humans. Cancer Res. *61*, 6649–6655.

Chen, H.X., and Cleck, J.N. (2009). Adverse effects of anticancer agents that target the VEGF pathway. Nat. Rev. Clin. Oncol. *6*, 465–477.

Cullen, M., Seaman, S., Chaudhary, A., Yang, M.Y., Hilton, M.B., Logsdon, D., Haines, D.C., Tessarollo, L., and St. Croix, B. (2009). Host-derived tumor endothelial marker 8 promotes the growth of melanoma. Cancer Res. *69*, 6021–6026.

Cullen, M., Elzarrad, M.K., Seaman, S., Zudaire, E., Stevens, J., Yang, M.Y., Li, X., Chaudhary, A., Xu, L., Hilton, M.B., et al. (2011). GPR124, an orphan G protein-coupled receptor, is required for CNS-specific vascularization and establishment of the blood-brain barrier. Proc. Natl. Acad. Sci. USA *108*, 5759–5764.

Dallas, N.A., Fan, F., Gray, M.J., Van Buren, G., II, Lim, S.J., Xia, L., and Ellis, L.M. (2007). Functional significance of vascular endothelial growth factor receptors on gastrointestinal cancer cells. Cancer Metastasis Rev. *26*, 433–441.

Drixler, T.A., Vogten, M.J., Ritchie, E.D., van Vroonhoven, T.J., Gebbink, M.F., Voest, E.E., and Borel Rinkes, I.H. (2002). Liver regeneration is an angiogenesis-associated phenomenon. Ann. Surg. *236*, 703–711, discussion 711–712.

Du, R., Lu, K.V., Petritsch, C., Liu, P., Ganss, R., Passegué, E., Song, H., Vandenberg, S., Johnson, R.S., Werb, Z., and Bergers, G. (2008). HIF1α induces the recruitment of bone marrow-derived vascular modulatory cells to regulate tumor angiogenesis and invasion. Cancer Cell *13*, 206–220.

Duan, H.F., Hu, X.W., Chen, J.L., Gao, L.H., Xi, Y.Y., Lu, Y., Li, J.F., Zhao, S.R., Xu, J.J., Chen, H.P., et al. (2007). Antitumor activities of TEM8-Fc: an engineered antibody-like molecule targeting tumor endothelial marker 8. J. Natl. Cancer Inst. *99*, 1551–1555.

Eremina, V., Cui, S., Gerber, H., Ferrara, N., Haigh, J., Nagy, A., Ema, M., Rossant, J., Jothy, S., Miner, J.H., and Quaggin, S.E. (2006). Vascular endothelial growth factor A signaling in the podocyte-endothelial compartment is required for mesangial cell migration and survival. J. Am. Soc. Nephrol. *17*, 724–735.

Felicetti, P., Mennecozzi, M., Barucca, A., Montgomery, S., Orlandi, F., Manova, K., Houghton, A.N., Gregor, P.D., Concetti, A., and Venanzi, F.M. (2007). Tumor endothelial marker 8 enhances tumor immunity in conjunction with immunization against differentiation Ag. Cytotherapy *9*, 23–34.

Fernando, S., and Fletcher, B.S. (2009). Targeting tumor endothelial marker 8 in the tumor vasculature of colorectal carcinomas in mice. Cancer Res. *69*, 5126–5132.

Gerber, H.P., Condorelli, F., Park, J., and Ferrara, N. (1997). Differential transcriptional regulation of the two vascular endothelial growth factor receptor genes. Flt-1, but not Flk-1/KDR, is up-regulated by hypoxia. J. Biol. Chem. *272*, 23659–23667.

Jinnin, M., Medici, D., Park, L., Limaye, N., Liu, Y., Boscolo, E., Bischoff, J., Vikkula, M., Boye, E., and Olsen, B.R. (2008). Suppressed NFAT-dependent VEGFR1 expression and constitutive VEGFR2 signaling in infantile hemangioma. Nat. Med. *14*, 1236–1246.

Kerbel, R.S. (2008). Tumor angiogenesis. N. Engl. J. Med. *358*, 2039–2049.

Lamszus, K., Ulbricht, U., Matschke, J., Brockmann, M.A., Fillbrandt, R., and Westphal, M. (2003). Levels of soluble vascular endothelial growth factor (VEGF) receptor 1 in astrocytic tumors and its relation to malignancy, vascularity, and VEGF-A. Clin. Cancer Res. *9*, 1399–1405.

Liu, S., Wang, H., Currie, B.M., Molinolo, A., Leung, H.J., Moayeri, M., Basile, J.R., Alfano, R.W., Gutkind, J.S., Frankel, A.E., et al. (2008). Matrix metalloproteinase-activated anthrax lethal toxin demonstrates high potency in targeting tumor vasculature. J. Biol. Chem. *283*, 529–540.

Liu, S., Crown, D., Miller-Randolph, S., Moayeri, M., Wang, H., Hu, H., Morley, T., and Leppla, S.H. (2009). Capillary morphogenesis protein-2 is the major receptor mediating lethality of anthrax toxin in vivo. Proc. Natl. Acad. Sci. USA *106*, 12424–12429.

Maharaj, A.S., and D'Amore, P.A. (2007). Roles for VEGF in the adult. Microvasc. Res. *74*, 100–113.

Masood, R., Cai, J., Zheng, T., Smith, D.L., Hinton, D.R., and Gill, P.S. (2001). Vascular endothelial growth factor (VEGF) is an autocrine growth factor for VEGF receptor-positive human tumors. Blood *98*, 1904–1913.

Nanda, A., Carson-Walter, E.B., Seaman, S., Barber, T.D., Stampfl, J., Singh, S., Vogelstein, B., Kinzler, K.W., and St. Croix, B. (2004). TEM8 interacts with the cleaved C5 domain of collagen α 3(VI). Cancer Res. *64*, 817–820.

Natsume, A., Niwa, R., and Satoh, M. (2009). Improving effector functions of antibodies for cancer treatment: enhancing ADCC and CDC. Drug Des. Devel. Ther. *3*, 7–16.

Oosthuyse, B., Moons, L., Storkebaum, E., Beck, H., Nuyens, D., Brusselmans, K., Van Dorpe, J., Hellings, P., Gorselink, M., Heymans, S., et al. (2001). Deletion of the hypoxia-response element in the vascular endothelial growth factor promoter causes motor neuron degeneration. Nat. Genet. *28*, 131–138.

Reeves, C.V., Dufraine, J., Young, J.A., and Kitajewski, J. (2010). Anthrax toxin receptor 2 is expressed in murine and tumor vasculature and functions in endothelial proliferation and morphogenesis. Oncogene *29*, 789–801.

Rouleau, C., Menon, K., Boutin, P., Guyre, C., Yoshida, H., Kataoka, S., Perricone, M., Shankara, S., Frankel, A.E., Duesbery, N.S., et al. (2008). The systemic administration of lethal toxin achieves a growth delay of human melanoma and neuroblastoma xenografts: assessment of receptor contribution. Int. J. Oncol. *32*, 739–748.

Ruan, Z., Yang, Z., Wang, Y., Wang, H., Chen, Y., Shang, X., Yang, C., Guo, S., Han, J., Liang, H., and Wu, Y. (2009). DNA vaccine against tumor endothelial marker 8 inhibits tumor angiogenesis and growth. J. Immunother. *32*, 486–491.

Scobie, H.M., Rainey, G.J., Bradley, K.A., and Young, J.A. (2003). Human capillary morphogenesis protein 2 functions as an anthrax toxin receptor. Proc. Natl. Acad. Sci. USA *100*, 5170–5174.

Seaman, S., Stevens, J., Yang, M.Y., Logsdon, D., Graff-Cherry, C., and St. Croix, B. (2007). Genes that distinguish physiological and pathological angiogenesis. Cancer Cell *11*, 539–554.

Shojaei, F., Wu, X., Malik, A.K., Zhong, C., Baldwin, M.E., Schanz, S., Fuh, G., Gerber, H.P., and Ferrara, N. (2007). Tumor refractoriness to anti-VEGF treatment is mediated by CD11b^{+}Gr1^{+} myeloid cells. Nat. Biotechnol. *25*, 911–920.

St. Croix, B., Rago, C., Velculescu, V., Traverso, G., Romans, K.E., Montgomery, E., Lal, A., Riggins, G.J., Lengauer, C., Vogelstein, B., and

Kinzler, K.W. (2000). Genes expressed in human tumor endothelium. Science *289*, 1197–1202.

Sung, H.K., Michael, I.P., and Nagy, A. (2010). Multifaceted role of vascular endothelial growth factor signaling in adult tissue physiology: an emerging concept with clinical implications. Curr. Opin. Hematol. *17*, 206–212.

Verheul, H.M., and Pinedo, H.M. (2007). Possible molecular mechanisms involved in the toxicity of angiogenesis inhibition. Nat. Rev. Cancer *7*, 475–485.

Werner, E., Kowalczyk, A.P., and Faundez, V. (2006). Anthrax toxin receptor 1/tumor endothelium marker 8 mediates cell spreading by coupling extracellular ligands to the actin cytoskeleton. J. Biol. Chem. *281*, 23227–23236.

Yamaguchi, T., Bando, H., Mori, T., Takahashi, K., Matsumoto, H., Yasutome, M., Weich, H., and Toi, M. (2007). Overexpression of soluble vascular endothelial growth factor receptor 1 in colorectal cancer: association with progression and prognosis. Cancer Sci. *98*, 405–410.

Yang, F., Jin, C., Jiang, Y.J., Li, J., Di, Y., and Fu, D.L. (2011a). Potential role of soluble VEGFR-1 in antiangiogenesis therapy for cancer. Expert Rev. Anticancer Ther. *11*, 541–549.

Yang, M.Y., Chaudhary, A., Seaman, S., Dunty, J., Stevens, J., Elzarrad, M.K., Frankel, A.E., and St. Croix, B. (2011b). The cell surface structure of tumor endothelial marker 8 (TEM8) is regulated by the actin cytoskeleton. Biochim. Biophys. Acta *1813*, 39–49.

Yang, X., Zhu, H., and Hu, Z. (2010). Dendritic cells transduced with TEM8 recombinant adenovirus prevents hepatocellular carcinoma angiogenesis and inhibits cells growth. Vaccine *28*, 7130–7135.